

# MERIDIONAL MIXING IN MARS NORTH POLAR REGION.

A. L. Sprague, W. V. Boynton, D. M. Hunten, *Lunar and Planetary Laboratory, AZ*, R. R. Reedy, *University of New Mexico, NM*, A. E. Metzger, *Jet Propulsion Laboratory, CA*.

## Introduction

We present measurements of Ar in Mars' atmosphere obtained with the Gamma Subsystem (GS) of the suite of three instruments comprising the Gamma Ray Spectrometer (GRS) on 2001 Mars Odyssey spacecraft [Boynton et al. 2004]. The data set discussed extends from early in the mapping orbit, 8 June 2002 to 2 April 2005. We follow the convention of arbitrarily numbering consecutive Mars Years (MY) from 11 April 1955 (beginning MY 01) following Clancy et al. [2000]. Time periods are given in terms of areocentric longitude of Mars ( $L_s$ ), where  $L_s = 0^\circ$  is defined as the vernal equinox for the northern hemisphere. In this reference frame, the GRS began mapping at  $L_s = 24.2^\circ$ . Because data are binned in time to build meaningful statistics (a high signal-to-noise ratio), the first data point for Ar is  $L_s = 27.2^\circ$ . The total time span covered in this paper is  $L_s = 24.2^\circ$ , MY 26 to  $L_s = 187.5^\circ$ , MY 27. There is no similar strong enhancement of Ar over north-polar regions during northern winter that was reported by Sprague et al. [2004] for southern winter. Part of this difference is explained by the global topographic dichotomy and the fact that the duration of northern autumn and winter is only 80% as long as that of southern autumn and winter.

The GS integrates  $\gamma$ -ray line emission at 1294 keV generated by the decay of  $^{41}\text{Ar}$  created when a thermal neutron is captured by  $^{40}\text{Ar}$  in Mars' atmosphere. As with all the useful  $\gamma$ -ray lines in the energy range of the GS, they are summed over time and binned in latitude and longitude sectors after the signal is transmitted from the spacecraft to the laboratory. Details of the computation of the footprint, data collection, binning, and processing, for Ar and the suite of other elemental emissions, can be found in Boynton et al. [2002, 2005] and Evans et al. [2002, 2005].

The Mars' atmospheric Ar data set is produced by deducing the amount of Ar in Mars' atmosphere within the footprint of the GS as it orbits Mars. The GS, on the 6-meter extended boom of the spacecraft, is at a nearly constant distance from the center of Mars and 99% of the  $\gamma$ -ray signal comes from within a region defined by a  $17^\circ$  half angle with vertex at the center of the planet. This geometry defines a footprint region approximately 2000 km diameter. The actual footprint varies somewhat because atmospheric attenuation decreases the footprint as energy of  $\gamma$ -rays decreases. The 1294 keV  $\gamma$ -ray line is generated in the atmosphere rather than in surface materials and the footprint may not be that of  $\gamma$ -rays of comparable energy emanating from surface materials [Masarik and Reedy 1996]. However, the scale height

of Mars' atmosphere is small (10 km) compared to the altitude of the spacecraft (400 km) so approximately the same footprint can be assumed.

Results from an analysis of atmospheric Ar for the autumn, winter and spring seasons over the south-polar region ( $75^\circ\text{ S}$  to  $90^\circ\text{ S}$ ) have been reported previously [Sprague et al. 2004]. Argon was observed to increase steadily throughout autumn, begin to decrease at the onset of winter and then to reach a minimum in early spring. By summer, Ar abundance was at the level expected from the value measured by the Viking Lander II (VL2) mass spectrometer [Biemann et al. 1976, Owen and Bieman 1976, Owen et al. 1977]. Sprague et al. [2004] used Ar as an atmospheric tracer and computed meridional mixing efficiencies in and out of the south-polar region. Mixing efficiency was found to be slow in autumn and the enhancement of Ar to a factor of 6 over the VL2 value was a consequence. More rapid mixing out of the south polar region in winter diminished the enhancement. In spring, when gaseous  $\text{CO}_2$  sublimed off the southern polar cap, rapid dilution of Ar occurred lowering the mixing ratio.

## North Polar Winter Argon Enhancement

Here we report measurements and computations of north polar meridional mixing. Mars' atmospheric Ar abundance measured by the GS has been calculated in a  $15^\circ$  increment in  $L_s$  and circum-planet zonal band of  $15^\circ$  in latitude ( $75^\circ\text{ N}$  to  $90^\circ\text{ N}$ ). According to the GS north polar data set, the Ar abundance may peak in northern winter with an enhancement factor of three. In Fig. 1 we show the GRS GS data before (grey) and after (black) a 3 pt boxcar smooth. Also shown is the mass of Ar expected from simply multiplying the ARC GCM seasonal atmospheric mass [Haberle et al. 1993] over the  $75^\circ\text{ N}$  to  $90^\circ\text{ N}$  polar region by the VL2 measured mass mixing ratio (0.0145).

An interpolation of the model of the seasonally adjusted Ar mixing ratio for the north polar atmosphere is also shown (grey solid line). It was computed by multiplying the MGCM seasonal  $\text{CO}_2$  column mass density by 0.0145 (the mass mixing ratio measured by VL2) and then normalizing each value to the mass column density at the location and season of the VL2 measurement.

Measurements made by the Neutron Spectrometer (NS) of thermal and epithermal counting rates over the northern polar region were reported by Feldman et al. [2003]. Lower thermal counting rates during autumn than during the period following the onset of polar cap

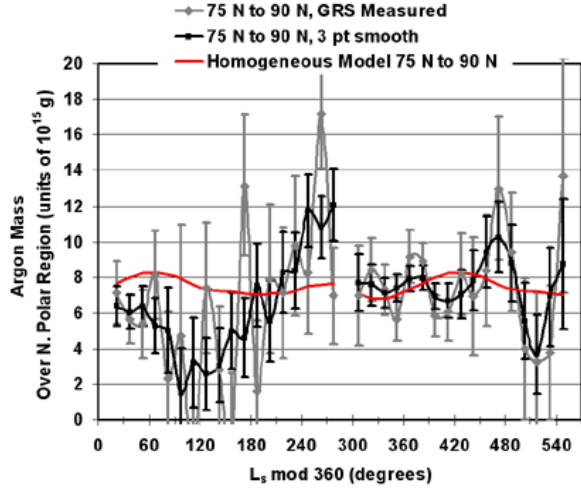


Figure 1: North polar (75° N to 90° N) Ar mass (grey line with error bars) as measured by the GRS compared to the same data with a 3 pt boxcar smooth (black line with error bars) and to the homogeneous Ar model in which the ARC GCM atmospheric thicknesses are multiplied by the measured VL2 mass mixing ratio of 0.0145 (undulating line with values near 8).

sublimation indicate higher Ar and N<sub>2</sub> concentrations as the polar frost cap forms than after the cap begins to sublime. The magnitude of the effect was estimated through the use of MCNPX simulations [Waters 1999] and with an effective non-condensable fraction of 3.3% for the baseline atmosphere. Based on the decreasing (during autumn) and increasing (during winter) thermal neutron counting rates they estimate changes in the Ar + N<sub>2</sub> of +15% and -18% respectively, relative to the normal Ar + N<sub>2</sub> value. The behavior of Ar and N<sub>2</sub> deduced by Feldman et al. [2003] for the north-polar region is qualitatively similar to that found in this analysis for Ar alone.

The topographically low northern region has nearly double the amount of atmospheric CO<sub>2</sub> in a column as the south polar region. This dilutes the non-condensable enhancement. The temporal variations of the enhancement curves between the two polar regions are also notably different. Enhancement in the south-polar region rises and declines as a relatively smooth function of time. Enhancement begins soon after the onset of autumn and peaks near L<sub>s</sub> = 110°. In the north, the data exhibit fluctuations; some may be statistically significant. If they are, they suggest greater eddy mixing. Mars GCM analyses [Barnes et al. 1993; Barnes 1996a] indicate Mars north-polar region is better connected to the global atmospheric system than the south-polar region. Baroclinic wave activity is strong near the winter solstice in the high latitudes of the northern hemisphere (much more so than in the southern hemisphere during winter solstice).

Thus, heat and mass transfer is efficient [Banfield et al., 2004]. Steeper topographical slopes [Thomas et al. 2000] in the southern hemisphere weaken eddy mixing near the pole [Barnes et al., 1993], helping to induce a strong seasonal peak in non-condensable enhancement. Also, northern winter occurs during perihelion; it is both warmer and shorter in duration, reducing the cumulative effect of the north polar CO<sub>2</sub> condensation and the north polar enhancement.

### North Polar Meridional Transport

We address the horizontal transport made apparent in the GS data by using a formulation of the flux of Ar into and out of the northern polar latitudes (75° N to 90° N).

The flux of Ar,  $F_1$ , (constituent 1) is:

$$F_1 = v_x \rho f_1 - K_x \rho \frac{df_1}{dx} \quad (1)$$

where  $\rho$  is the average martian atmosphere mass density,  $f_1$  is the Ar seasonal mass mixing ratio of the ambient martian air, equatorward, at mixing distance  $\Delta x$ , and  $v_x$  is the north-south wind speed. We take all parameters to be positive toward the north pole.

The first term on the right hand side of (1) is the condensation flow or flux of Ar, entrained in air (primarily CO<sub>2</sub>) moving toward the pole from low latitudes as the seasonal cap forms in autumn and winter. This movement of air constitutes a small southerly (from the south) wind (direction  $x$ ) with velocity  $v_x$  sustained throughout the period of CO<sub>2</sub> frost precipitation from L<sub>s</sub> = 180° to L<sub>s</sub> = 360°. In spring the direction of the wind changes and  $v_x$  becomes northerly. The first term then becomes the flux of entrained Ar moving toward the equator as the seasonal CO<sub>2</sub> cap rapidly sublimates in spring.

The condensation flow is offset by a second process at work to remove Ar from the high latitude region, even as it is accumulating in Autumn and Winter. This is expressed in the second term which describes the flux of Ar transported in and out of the north polar regions by the gradient in the mixing ratio and by deviations from the mean winds. This term is usually called eddy transport or eddy mixing.

The net flux  $F_1$  is the sum of both terms in (1). For computational convenience we estimate  $df_1/dx$  by  $\Delta f_1/\Delta x$  where  $\Delta f_1$  is the difference between the Ar mixing ratios measured by the GS within the north polar region and the ambient air a distance  $\Delta x$  away. We define this distance as that which Ar must be transported to no longer be observed in the north polar footprint of the GS and where the ambient seasonal mixing ratio can be reasonably estimated. A good approximation is an arc length equivalent to 30° of latitude.

A useful parameterization of mixing air by both processes in equation (1) is made by solving it for  $K_x$ , the horizontal eddy mixing coefficient. We compute the

value of  $K_x$  for every 15 deg increment of  $L_s$  using a rearrangement of (1):

$$K_x = \frac{\Delta x}{\Delta f_1} (v_x f_1 - \frac{F_1}{\rho}). \quad (2)$$

With our choice of signs, an equatorward total Ar flux  $F_1$  is negative, and this is the case throughout autumn and winter.

We make several computations of meridional mixing, for 15° intervals of  $L_s$  throughout autumn, winter, and spring. The flux of Ar atoms in to or out of the polar region  $F_1$ , is found using the actual GS measurements by calculating the mass of Ar passing through a cylindrical region with radius corresponding to a 75° latitude circle. The mass of Ar lost from the region is the difference between the model prediction (after taking into account the apparent loss during the preceding time periods) and the GS measurements. Duration of flow is the time in each 15° increment of  $L_s$ . The gradient in mixing ratios ( $\Delta f_1$ ) is obtained from the difference of the measured mixing ratio and the estimated seasonally adjusted mixing ratio of the ambient martian air outside of the polar region at 45°N.

A peak in Ar has been reached by the onset of Winter. From that time on the mixing ratio drops even though Ar enrichment continues as CO<sub>2</sub> frost is precipitating on the north polar cap until the end of winter [Pollack et al. 1990; Kelly et al. 2005]. That the Ar mixing ratio does not continue to increase throughout this period is because of variable equatorward mixing.

The mixing style in the north is clearly different than that of the south (see Sprague et al. 2004). The transport of Ar owing to the gradient in the mixing ratio and fluctuations in the mean winds (eddy mixing) is variable. The direction of flow appears to switch several times during the autumn, winter and spring. The magnitude of the mixing changes notably with time, possibly indicating effects of wave induced eddies [Murphy et al. 1995; Barnes et al 1996 a,b; Wilson et al. 2002; Banfield 2004].

### Acknowledgments:

We acknowledge the contributions of the entire GRS team, Bob Haberle for providing great discussion and the NASA ARC MGCM output 2002.17 for analysis purposes, and funding from NASA contract no. 1228726.

### References:

Banfield, D., B.J. Conrath, P.J. Gierasch, R.J. Wilson, and M.D. Smith (2004), Traveling waves in the martian atmosphere from MGS TES Nadir data, *Icarus*, 170, 365-403.

Barnes, J.R., J.B. Pollack, R.M. Haberle, C.B. Leovy, R.W. Zurek, H. Lee, and J. Schaeffer (1993), Mars atmospheric dynamics as simulated by the NASA AMES General Circulation Model. II - Transient baroclinic eddies, *J. Geophys. Res.*, 98, 3125-3148.

Barnes, J.R., R.M. Haberle, J.B. Pollack, H. Lee, and J. Schaeffer (1996a), Mars atmospheric dynamics as simulated by the NASA Ames general circulation model 3. Winter quasi-stationary, *J. Geophys. Res.*, 101, 12753-12776.

Barnes, J.R., T.D. Walsh, and J.R. Murphy (1996b), Transport timescales in the Martian atmosphere: General circulation model simulations, *J. Geophys. Res.*, 101, 16881-16890.

Biemann, K., A.L. Lafleur, T. Owen, D.R. Rushneck, and D.W. Howarth (1976), The atmosphere of Mars near the surface - Isotope ratios and upper limits on noble gases, *Science*, 194, 76-78.

Boynton, W.V., W.C. Feldman, I. Mitrofanov, L.G. Evans, R.C. Reedy, S.W. Squyres, R. Starr, J.I. Trombka, C. d'Uston, J.R. Arnold, J. Englert, A.E. Metzger, H. Wanke, J. Bruckner, D.M. Drake, C. Shinohara, C. Fellows, D.K. Hamara, K. Harshman, K. Kerry, C. Turner, M. Ward, H. Barthe, K.R. Fuller, S.A. Storms, G.W. Thornton, J.S. Longmire, M.L. Litvak, and A.K. Ton'Chev (2004), The Mars Odyssey Gamma-Ray Spectrometer Instrument Suite, *Space Science Reviews*, 110, 37 - 83.

Boynton, W.V., L.G. Evans, R. C. Reedy, R. Starr, A. E. Metzger, I. Mitrofanov, J. I. Trombka, C. d'Uston, H. Wanke, O. Gasnault, D. K. Hamara, D. M. Janes, R. L. Marcialis, S. Maurice, G. J. Taylor (2005), Data Analysis of the GRS GS instrument, *J. Geophys. Res.*, submitted.

Evans, L.G., R. C. Reedy, R. D. Starr, W.V. Boynton, and J.I. Trombka (2002), Background lines in the Mars Odyssey 2001 gamma-ray detector, in *SPIE, International Society for Optical Engineering*, edited by R.B. James, L.A. Franks, A. Burger, E.M. Westbrook, and R.D. Durst, 31-44.

Evans, L.G., R.C. Reedy, R.D. Starr, K. E. Kerry and W.V. Boynton (2005), Analysis of Gamma-Ray Spectra Measured by Mars Odyssey. *J. Geophys Res.*, submitted.

Feldman, W.C., T.H. Prettyman, W.V. Boynton, J.R. Murphy, S. Squyres, S. Karunatillake, S. Maurice, R.L. Tokar, G.W. McKinney, D.K. Hamara, N. Kelly, and K. Kerry (2003), CO<sub>2</sub> frost cap thickness on Mars during northern winter and spring, *J. Geophys. Res.*, 108i, 7-1.

Haberle, R.M., J.B. Pollack, J.R. Barnes, R.W. Zurek, C.B. Leovy, J.R. Murphy, H. Lee, and J. Schaeffer (1993), Mars atmospheric dynamics as simulated by the NASA AMES General Circulation Model. I - The zonal-mean circulation, *J. Geophys. Res.*, 98, 3093-3123.

Kelly, N.J., W.V. Boynton, K. Kerry, D. Hamara, D. Janes, R.C. Reedy, K.J. Kim, R.M. Haberle, and the GRS Team (2005). Seasonal Polar Carbon Diox-

North Polar Meridional Mixing: Sprague et al.

ide Frost on Mars: Spatiotemporal Dependence of CO<sub>2</sub> Thickness and Mass as Determined from 2001 Mars Odyssey Gamma Ray Spectrometer Data, *J. Geophys Res.*, submitted.

Masarik, J., and R.C. Reedy (1996), Gamma ray production and transport in Mars, *J. Geophys Res.*, 101(E8), 18,891-18,912.

Murphy, J.R., J.B. Pollack, R.M. Haberle, C.B. Leovy, O.B. Toon, and J. Schaeffer (1995), Three-dimensional numerical simulation of Martian global dust storms, *J. Geophys Res.*, 100(E12), 26357-26376  
DOI: 10.1029/95JE02984.

Owen, T., and K. Biemann (1976), Composition of the atmosphere at the surface of Mars - Detection of argon-36 and preliminary analysis, *Science*, 193, 801-803.

Owen, T., K. Biemann, D.R. Rushneck, J.E. Biller, D.W. Howarth, and A.L. Lafleur (1977), The Composition of the Atmosphere at the Surface of Mars, *J. Geophys Res.*, 82(28), 4635-4639.

Pollack, J.B., R.M. Haberle, J. Schaeffer, and H.

Lee (1990), Simulations of the general circulation of the Martian atmosphere: I - Polar processes, *J. Geophys. Res.*, 95, 1447-1473.

Sprague, A.L., W.V. Boynton, K.E. Kerry, D.M. Janes, D.M. Hunten, K.J. Kim, R.C. Reedy, and A.E. Metzger (2004), Mars' South Polar Ar Enhancement: A Tracer for South Polar Seasonal Meridional Mixing, *Science*, 306(19 November), 1364 - 1367.

Thomas, P.C., M.C. Malin, K.S. Edgett, M.H. Carr, W.K. Hartmann, A.P. Ingersoll, P.B. James, L.A. Soderblom, J. Veverka, and R. Sullivan (2000), North-south geological differences between the residual polar caps on Mars, *Nature*, 404(6774), 161-164.

Waters, L.S. (1999), MCNPX User's Guide, Los Alamos Natl. Lab., Report LA-UR-99. Los Alamos, NM.

Wilson, R.J., D. Banfield, B.J. Conrath, and M.D. Smith (2002), Traveling waves in the Northern Hemisphere of Mars, *Geophys. Res. Lett.*, 29(14), 29-1, Cite ID 1684, DOI 10.1029/2002GL014866.